

# Response of NaI(Tl) to Energetic Heavy Ions\*

E. NEWMAN† AND F. E. STEIGERT  
Yale University, New Haven, Connecticut

(Received January 22, 1960)

The light output of NaI(Tl) was measured as a function of energy for ions of  $\text{He}^4$ ,  $\text{B}^{10}$ ,  $\text{B}^{11}$ ,  $\text{C}^{12}$ ,  $\text{N}^{14}$ ,  $\text{O}^{16}$ ,  $\text{F}^{19}$ , and  $\text{Ne}^{20}$  from approximately 1.0 to 10.0 Mev/nucleon. The particle energy was varied with absorbing foils and the degraded beam analyzed in a magnetic spectrometer. Light output becomes linear with energy above approximately 6 Mev/amu. There appears to be an odd-even incident charge effect in the saturation value of the differential efficiency of fluorescence,  $dL/dE$ .

## INTRODUCTION

THE use of scintillation crystals as particle detectors has been well established over the past decade. Their behavior with respect to light particles has already been adequately covered.<sup>1,2</sup> Knowledge of the response for ion species heavier than alphas is, by contrast, somewhat more restricted. Only  $\text{CsI}^{3-5}$  and  $\text{KI}^6$  have been reported. There are, however, many experiments involving heavy ions where the high luminous efficiency of NaI outweighs the problems posed by its hygroscopic properties.

All of the measurements of light output have demonstrated a nonlinearity at low and intermediate energies. This behavior has usually been attributed to saturation effects in the crystal for high specific energy loss. This investigation is particularly well suited to examine the fluorescence efficiency in the region of very large  $dE/dx$ .

## EXPERIMENTAL METHOD

Ion beams of  $\text{He}^4$ ,  $\text{B}^{10}$ ,  $\text{B}^{11}$ ,  $\text{C}^{12}$ ,  $\text{N}^{14}$ ,  $\text{O}^{16}$ ,  $\text{F}^{19}$ , and  $\text{Ne}^{20}$  at a nominal energy of 10 Mev/amu were obtained from the Yale heavy ion linear accelerator. The experimental arrangement is shown in Fig. 1. The ions, upon leaving the accelerating cavity were magnetically analyzed and then scattered through a small angle from a gold foil of approximately 2.2 mg/cm<sup>2</sup>. This served to reduce the incident beam intensity so as to provide reasonable counting rates without danger of pile up or crystal fatigue. This foil was oriented normal to the incident beam axis. At a distance of 30 cm beyond this gold target an absorber wheel containing either aluminum or nickel foils was used to degrade the beam energy. On occasion the absorber wheel was removed and replaced by a gas cell with nickel end windows. Immediately beyond the energy degrader was placed

a pair of 0.005-inch wide vertical beam collimating slits optically aligned on the center of the gold target foil and defining a scattering angle of about 2°. These slits were contained within a magnetic shield of laminated iron, which brought the ion beam through the fringing field to within  $\frac{1}{2}$  inch of the flat field region of the magnet. The second of these slits served as the entrance port to the spectrometer. A third slit, 0.006 inch wide, was placed at the exit port of the spectrometer, still well within the flat field region. This apparatus and its alignment and calibration are discussed in more detail by Roll and Steigert<sup>7</sup> and Northcliffe.<sup>8</sup>

The ions, having traversed a path of known deflection within the spectrometer, now entered the detection system. Here two alternate methods of observation were available. In the forward section, nuclear emulsions could be inserted into the ion trajectory for exposure and then withdrawn. The scintillation detector used in this study was placed in the second section. This

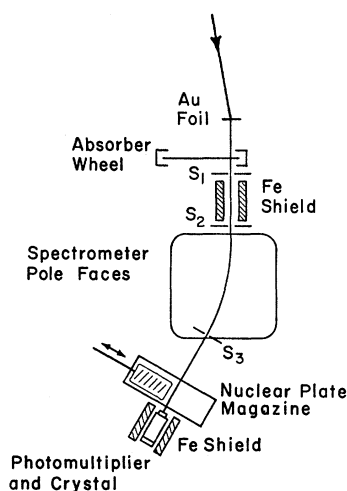


FIG. 1. Experimental arrangement for the measurement of the pulse height of the degraded heavy ions. The absorber wheel contained Al or Ni foils.  $S_1$ ,  $S_2$ ,  $S_3$  are vertical slits of 5-mil, 5-mil, and 6-mil widths, respectively. The nuclear emulsions may be inserted or removed at will.

\* Supported in part by the Office of Naval Research and the U. S. Atomic Energy Commission.

† Socony Mobil Fellow, 1959-60.

<sup>1</sup> F. S. Eby and W. K. Jentschke, Phys. Rev. **96**, 911 (1954).

<sup>2</sup> C. J. Taylor, W. K. Jentschke, M. E. Remley, F. S. Eby, and P. G. Kruger, Phys. Rev. **84**, 1034 (1951).

<sup>3</sup> A. R. Quinton, C. E. Anderson, and W. J. Knox, Phys. Rev. **115**, 886 (1959).

<sup>4</sup> S. Bashkin, R. R. Carlson, R. A. Douglas, and J. A. Jacobs, Phys. Rev. **109**, 434 (1958).

<sup>5</sup> M. L. Halbert, Phys. Rev. **107**, 647 (1957).

<sup>6</sup> W. E. Burcham, Proc. Phys. Soc. (London) **A76**, 309 (1957).

<sup>7</sup> P. G. Roll and F. E. Steigert, Nuclear Phys. (to be published); see also Bull. Am. Phys. Soc. **4**, 51 (1959).

<sup>8</sup> L. C. Northcliffe (to be published).

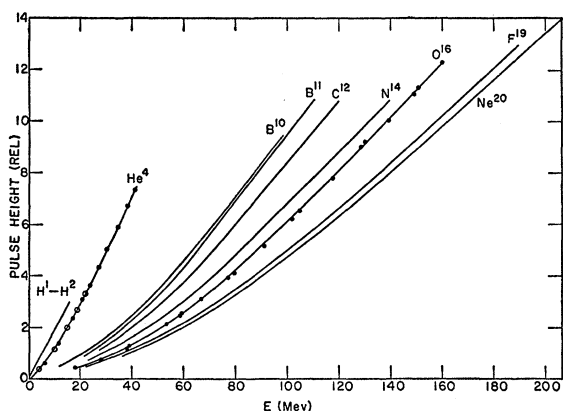


FIG. 2. Pulse height vs  $E$  for various heavy ions in NaI (Tl). Pulse height of the ThC' alpha=1.  $H^1$ ,  $H^2$ , and the open circles are data of reference 1.

section was enclosed within a laminated magnetic shield comprised of two iron cylinders and several layers of Co-netic sheet in order to minimize any stray field effects.

The crystal used was 0.5 in. in diameter by 1 mm thick. After careful cleaning and polishing in a dry box, the crystal was mounted directly to the face of a Du-Mont 6292 phototube with Dow-Corning silicone fluid. An aluminized plexiglass retainer with a collimating hole  $\frac{1}{4}$  inch in diameter and a step 0.001 in. shallower than the crystal was used to center and provide the "squeeze" required to keep the detector in good optical contact with the photomultiplier. The entire crystal-photomultiplier assembly with its associated potential divider string were located in a vacuum container which could be evacuated while in the dry box. This system could then be isolated with a circle seal valve for later assembly into the spectrometer. After the spectrometer was pumped down, the connecting valve could be opened. In this fashion the NaI crystal was always protected against moisture without recourse to packaging or use of windows. The high voltage and signal leads were brought out of the vacuum container to the power supply and White follower through Stupakoff seals.

Data points were obtained by degrading the full energy beam the desired amount by the use of appropriate absorbers. The output of the phototube was displayed after suitable amplification on an oscilloscope. A parallel signal was fed to a count rate meter. The magnetic field of the spectrometer was varied until a maximum in the counting rate was observed. The value of the magnetic field was determined by use of a proton or lithium resonance probe. Charge state identification was then made by demonstrating that the magnetic fields for the successive maxima were in the correct ratio. The spectrum was then analyzed using an Atomic 20 channel pulse-height analyzer. Typical counting rates were on the order of 400 counts/min. Counting

statistics of the order of 2% in the peak were obtained. No difference in the pulse height of various charge states was noted. Upon completion of a data point a nuclear emulsion was exposed. In this fashion one obtained additional confidence in the identification of the charge state and/or beam species by a cross comparison with the emulsion range energy data.<sup>7</sup>

At convenient intervals during a run, calibration was made using the 8.78-Mev alpha particle group from ThC'. This precaution was taken to guarantee that no pulse-height shift, outside the quoted error, occurred due to crystal fatigue, phototube high voltage or electronic drift. A further test, that of repeating runs with higher photomultiplier tube voltages, and comparing to similarly taken calibration runs, demon-

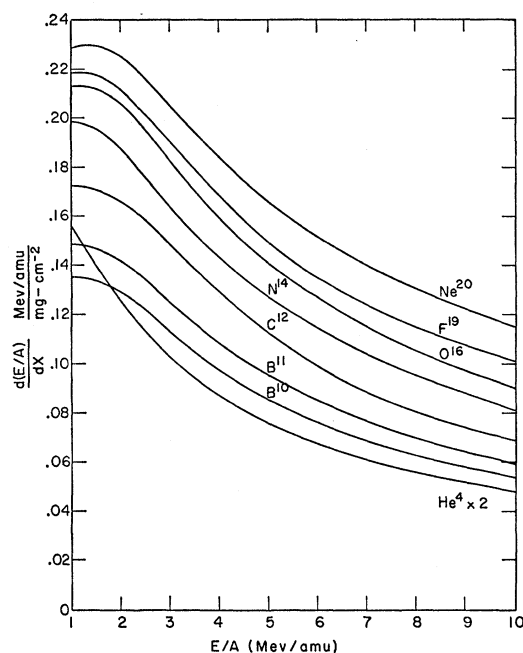


FIG. 3. Calculated values of the specific energy loss per nucleon as a function of the energy per nucleon for various heavy ions in NaI (Tl).

strated that the photomultiplier was not space charge limiting nor the electronics saturating.

## RESULTS AND DISCUSSION

The response of the scintillator to beams of  $He^4$ ,  $B^{10}$ ,  $B^{11}$ ,  $C^{12}$ ,  $N^{14}$ ,  $O^{16}$ ,  $F^{19}$ , and  $Ne^{20}$  is shown in Fig. 2. Experimental points are shown on the  $He^4$  and  $O^{16}$  curves and are omitted from the others to avoid confusion. The curves drawn represent the best smooth curve through the data. The  $H^1$  and  $H^2$  data of reference 1 is shown also for comparison. The  $He^4$  data obtained by these workers with the standard 0.0013 mole fraction of Tl is indicated by open circles. For the region above approximately 6.5 Mev/nucleon the pulse height appears to be linear in energy for all ions heavier than He.

All of the individual runs are normalized by taking the ratio of the observed pulse height to that of the ThC' alpha.

The resolution of the scintillator showed the characteristic inverse proportionality to the square root of energy in the linear region of the curves. An increase in the percent resolution with increasing particle mass was also observed. Typical resolutions at 10 Mev/nucleon were of the order of 3%. The resolutions quoted above permitted the determination of the pulse height to approximately  $\pm 1\%$  at high energies and to  $\pm 2\%$  at 2 Mev/nucleon. The error in  $E$  is of the order of 0.5%.

In order to obtain information on the saturation phenomenon one must know the specific energy loss in the scintillator. The curves of Northcliffe<sup>8</sup> and of Roll and Steigert<sup>7</sup> for the residual ranges of various heavy ions in aluminum, nickel, and oxygen were differentiated and used to predict the specific energy loss

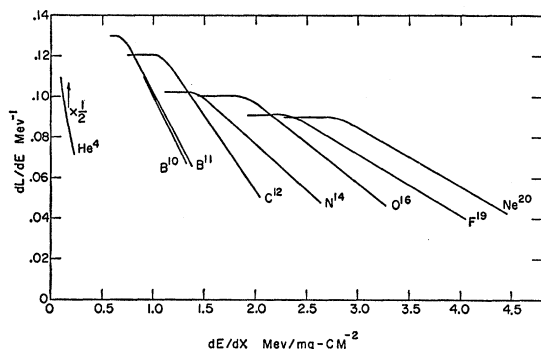


FIG. 4. The differential efficiency of fluorescence for NaI as a function of the specific energy loss.

in NaI. In making the extrapolation the expression,

$$\frac{d(E/A)}{\rho dx} \propto \left(\frac{Z'}{A'}\right) \ln\left(\frac{CE}{\bar{I}A}\right), \quad (1)$$

was used, where  $\rho$ ,  $A'$ ,  $Z'$  are the density, atomic number, and nuclear charge, respectively, of the stopping material and  $E/A$  is the energy per amu of the incident particle. The average ionization potential  $\bar{I}$  was taken to be  $13Z'$ .<sup>9</sup> For all ion species the agreement among the three curves ranged from better than 3% at full energy to about 10% for the slowest particles. Because of the nature of the approximations used and extrapolations made, no detailed adjustments of the curves were attempted. The average curve obtained is shown in Fig. 3. In view of the agreement among the individual curves this average is felt to have a relative accuracy of this same order. In absolute value, however, the curves could conceivably be systematically low by several percent, since, among other things, the

<sup>9</sup> R. Sternheimer, Phys. Rev. **115**, 137 (1959).

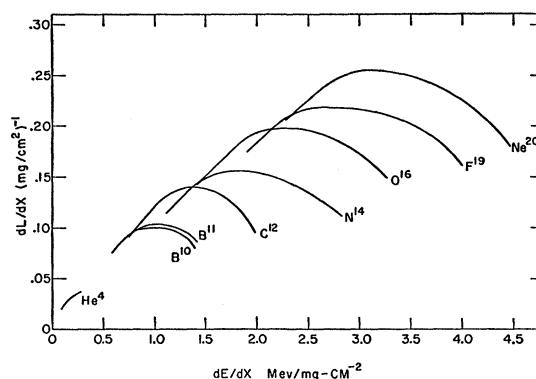


FIG. 5. The specific fluorescence as a function of the specific energy loss for various heavy ions in NaI.

source data was insensitive to energy losses via nuclear scattering, an approximation not valid here.

The differential efficiency of fluorescence ( $dL/dE$ ) is displayed as a function of the specific energy loss ( $dE/dx$ ) in Fig. 4. The respective regions of linearity (horizontal slope) and saturation are both quite apparent for all species. It is further evident that the demarcation between these two regions, denoting the onset of saturation, is occurring at increasingly larger values of  $dE/dx$  as one increases the mass and charge of the incident particle. Energy-wise, this knee occurs about 7-8 Mev/amu. It should be remembered that in all cases the energy increases to the left. The specific fluorescence ( $dL/dx$ ) is shown as a function of specific energy loss in Fig. 5. Again the region of linearity (constant slope) is quite apparent. For this linear region one may write

$$dL/dx = K dE/dx, \quad (2)$$

where the proportionality constant  $K$  varies with the ion species involved.

In Fig. 6 this coefficient has been plotted against the

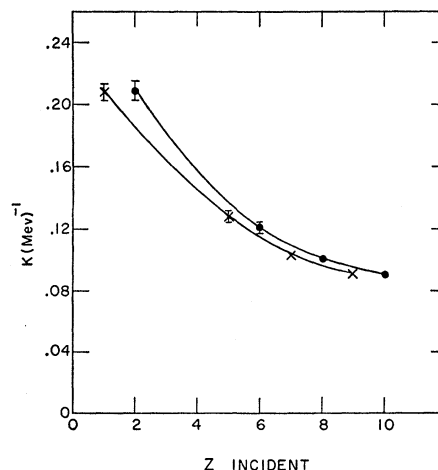


FIG. 6. The slope of the specific fluorescence vs specific energy loss for the high-energy linear portion as a function of the charge of the incident particle.

nuclear charge of the incident ion. One should probably have used the effective charge but in the region where Eq. (2) is valid no corrections were deemed necessary. One interesting feature of this plot is the odd-even charge effect. While these variations are within the extreme experimental errors for large  $Z$ , the even charge species appear to belong to a separate curve systematically above that of the odd charge group. For the purpose of illustration the two curves have been shown. The same sort of behavior is also suggested in

the saturation region. No obvious reason for such a splitting, if it is indeed real, can be offered at this time. The errors indicated are relative and for the larger  $Z$  ions the size of the point exceeds the estimated error. The absolute values of  $K$  may be in error by as much as 10%.

The authors wish to thank Mr. P. G. Roll for extensive assistance in obtaining this data. They also would like to acknowledge the loan of some equipment from Dr. L. C. Northcliffe.

## Nuclear Spin and Hyperfine Interaction of $\text{In}^{113m\ddagger}$

W. J. CHILDS AND L. S. GOODMAN  
Argonne National Laboratory, Lemont, Illinois  
(Received January 25, 1960)

The hyperfine structure of the 1.7-hr, 393-kev metastable state of  $\text{In}^{113}$  has been studied by use of the atomic-beam magnetic-resonance technique. The nuclear spin is found to be  $\frac{1}{2}$  and the magnetic dipole moment to be  $-0.21050 \pm 0.00002$  nm, subject to a possible hyperfine anomaly. The hyperfine separation in the atomic  $P_{\frac{1}{2}}$  state is measured to be  $781.084 \pm 0.010$  Mc/sec.

### INTRODUCTION

THE isotope  $\text{In}^{113}$  has long held the interest of nuclear physicists. The energy levels, the conversion coefficients, and the lifetime of the 393-kev isomeric state have received attention both from experimentalists<sup>1-6</sup> and theoreticians.<sup>7,8</sup>

A major triumph of the shell model of the nucleus was the explanation of such isomeric states. In the case of  $\text{In}^{113m}$ , the isomerism is described as being due to the existence of a large spin difference between the ground state, which has a measured spin of  $9/2$ ,<sup>9</sup> and the first excited state, for which the shell model predicts a spin of  $\frac{1}{2}$ . The ground state is assumed to arise from a proton hole in the  $g_{9/2}$  shell, the filling of which would complete the proton magic number 50. The isomeric state, according to the model, is due to the closely competing  $(p_{\frac{1}{2}})^1$  configuration.

The predicted spin difference of 4 is consistent with

the semiempirical rules<sup>10</sup> and theoretical treatments<sup>7,8</sup> of gamma-ray emission and electron conversion.

It is of interest to measure the spin of the excited state by a direct method and thus further confirm the theoretical predictions.

### THEORY OF THE METHOD

The Zeeman splitting of the hyperfine levels of the atomic  $P_{\frac{1}{2}}$  state was studied. The principles of the method have been so adequately described<sup>11,12</sup> that a complete review is unnecessary. It is desirable, however, in the interest of clarity, to set down a few pertinent concepts and equations used in interpreting the data.

In the scheme which Zacharias<sup>11</sup> originally applied in his studies of  $\text{K}^{40}$ , an atom in the atomic beam is successively deflected by two strong, inhomogeneous magnetic fields. These deflections are in the same direction unless an appropriate change of magnetic substate occurs between them. This change of state must be such that in the strong field of the second deflecting magnet the effective magnetic moment of the atom will be equal but of opposite sign to that in the first. Under this condition, the atom will be refocused through a slit where it can be detected. Suitable changes of state are induced by an appropriate radio-frequency field introduced into the gap of the homogeneous magnet. These observable transitions are indicated in the hyperfine diagram (Fig. 1).

<sup>†</sup> Work performed under the auspices of the U. S. Atomic Energy Commission.

<sup>1</sup> S. W. Barnes, Phys. Rev. **56**, 414 (1939).

<sup>2</sup> J. L. Lawson and J. M. Cork, Phys. Rev. **57**, 982 (1940).

<sup>3</sup> D. A. Thomas, S. K. Haynes, and C. D. Broyles, Phys. Rev. **82**, 961 (1951).

<sup>4</sup> T. B. Cook, Jr., and S. K. Haynes, Phys. Rev. **86**, 190 (1952).

<sup>5</sup> G. A. Graves, L. M. Langer, and R. D. Moffat, Phys. Rev. **88**, 344 (1952).

<sup>6</sup> S. B. Burson, H. A. Grench, and L. C. Schmid, Phys. Rev. **115**, 188 (1959).

<sup>7</sup> M. E. Rose, G. H. Goertzel, B. I. Spinrad, J. Harr, and P. Strong, Phys. Rev. **83**, 79 (1951).

<sup>8</sup> J. M. Blatt and V. F. Weisskopf, *Theoretical Nuclear Physics* (John Wiley and Sons, Inc., New York, 1952).

<sup>9</sup> D. A. Jackson, Z. Physik **80**, 59 (1933).

<sup>10</sup> M. Goldhaber and A. W. Sunyar, Phys. Rev. **83**, 906 (1951).

<sup>11</sup> J. R. Zacharias, Phys. Rev. **61**, 270 (1942).

<sup>12</sup> L. S. Goodman and S. Wexler, Phys. Rev. **99**, 192 (1955).